for faster-than-sound neutrons is (Willis & Pryor, 1975)

$$I_{\mathrm{TDS},\lambda} = \text{constant} \times (\sin^2\theta/\lambda^2) F^2 e^{-2M} k_B T. \quad (4)$$

Here F is the structure factor for Bragg scattering, e^{-2M} is the Debye-Waller factor (where $M = B\sin^2\theta/\lambda^2$) and T is the absolute temperature. The constant includes the elastic constants and the range of scan. Equation (4) is essentially unchanged for more realistic scans (Cooper, 1971).

Expression (4) is readily converted to the time-of-flight case by using the prescription of Buras & Gerward (1975). Thus

$$I_{\mathrm{TDS},t} = \text{constant} \times \varphi(\lambda)\lambda^2 F^2 e^{-2M} k_B T, \quad (5)$$

where $\varphi(\lambda)$ is the incident-beam intensity per unit wavelength range. If we plot

$$I_{\mathrm{TDS},t}/[\varphi(\lambda)\lambda^2 F^2 T]$$

on a logarithmic scale *versus* $\sin^2\theta/\lambda^2$, the points should lie on a straight line of slope $-2B$.

The measured data have been normalized to the incident flux $\varphi(\lambda)$, which was determined by monitoring the incident spectrum with a dilute ^{3}He detector and correcting for the variation of detector efficiency with neutron wavelength. Moreover, T is constant (293 K) and the structure factor F of silicon is the same for all reflections in the $hh0$ zone. Thus in Fig. 4 we have simply plotted $\ln(I_{\mathrm{TDS},t})/\varphi(\lambda)\lambda^2$ *versus* $\sin^2\theta/\lambda^2$.

At large values of $\sin^2\theta/\lambda^2$ the curves have a negative slope indicating $B \sim 0{\cdot}42$ Å^2, which is close to the accepted value, $B = 0{\cdot}46$ Å^2, quoted by Krec & Steiner (1984). However, as the wavelength increases and the neutron velocity falls below the velocity of sound in the crystal, there is a sharp fall-off in the integrated intensity I_{TDS} [as compared with that calculated from (5)]. The neutron velocity v is related to its wavelength by the de Broglie relation $\lambda = h/(m_n v)$. The lines L and T in Fig. 4 indicate the range of $\sin^2\theta/\lambda^2$ over which the neutron velocity lies between the maximum longitudinal (L) and minimum transverse (T) sound velocities. In the time-of-flight case the locus in reciprocal space for elastic scattering is a line along the reciprocal-lattice vector, unlike the fixed-wavelength case where this locus is the Ewald sphere. This line is at $90° - \theta$ to the scattered wave vector $\mathbf{k}$ and so a geometrical term, $\sec\theta$, is necessary in calculating the positions of L and T in Fig. 4. The sound velocities were calculated from the elastic constants given by McSkimin (1953).

The authors are especially grateful to Dr A. D. Taylor of the Rutherford Appleton Laboratory for his advice on shielding for the diffractometer. The computer programs used in the analysis were written by Mr A. S. Thornton and the silicon crystals were generously supplied by Mr N. W. Crick. We are also grateful for the expert help given us by the staff of the Helios linear accelerator and the Dido reactor at Harwell.

References

BURAS, B. & GERWARD, L. (1975). *Acta Cryst.* A31, 372-374.
BURAS, B. & LECIEJEWICZ, J. (1964). *Phys. Status Solidi*, 4, 349-355.
COOPER, M. J. (1971). *Acta Cryst.* A27, 148-157.
KREC, K. & STEINER, W. (1984). *Acta Cryst.* A40, 459-465.
LYNN, J. E. (1980). *Contemp. Phys.* 21, 483-500.
MCSKIMIN, H. J. (1953). *J. Appl. Phys.* 24, 988-997.
WILLIS, B. T. M. (1970). *Acta Cryst.* A26, 396-401.
WILLIS, B. T. M. & PRYOR, A. W. (1975). *Thermal Vibrations in Crystallography.* Cambridge Univ. Press.

Acta Cryst. (1986). A42, 191-197

The Intensity Fringes of Three Coupled Waves in Crystals

BY JOHANNES BREMER

Institutt for Røntgenteknikk, Universitetet i Trondheim-NTH, 7034 *Trondheim-NTH, Norway*

AND GUNNAR THORKILDSEN

Rogaland Distriktshøgskole, Ullandhaug, 4000 *Stavanger, Norway*

(*Received* 14 *August* 1985; *accepted* 26 *November* 1985)

Abstract

Two different kinds of interaction between three waves D_0, D_h and D_g in a perfect crystal are investigated in the case of Laue scattering using the Takagi-Taupin equations. Polarization effects (coupling between $\hat{\sigma}$ and $\hat{\pi}$ waves) are neglected, and it is assumed that the incoming vacuum wave $D_0^{(e)}$ has a small wave-front area whose spatial extension is simulated by a point source on the crystal surface. The solutions of the diffraction equations thus constitute the boundary-value Green functions for the wave

0108-7673/86/030191-07$01.50

fields. In the first case it is assumed that D_g is only indirectly coupled to D_0. In the second case energy is allowed to be exchanged between D_0 and D_h and between D_0 and D_g, but no D_h–D_g interaction is present. In both of these situations the field amplitudes are given by expressions that contain simple products of zeroth- and first-order Bessel functions. It is suggested that the intensity pattern can be observed directly. The transition to an incoming plane wave is outlined, and it is also demonstrated that the hyperbolic intensity fringes generated by two spherical waves can be deduced from the derived expressions.

Introduction

The probability of exciting more than two coupled waves is generally small when illuminating a crystal with X-rays. This is in pronounced contrast to high-energy electron diffraction where the shorter wavelength and correspondingly smaller Bragg angle increase the number of simultaneous overlaps between reciprocal-lattice points and the Ewald sphere. Nevertheless, three-beam diffraction has in X-ray crystallography recently found application as a method for retrieving the phases of reflections. The starting point for calculating intensities diffracted from mosaic crystals has to be the plane-wave theories that originally were developed for perfect crystals (Pinsker, 1978; Kato, 1974; Post, 1983; Chang, 1984).

We want in this paper to address ourselves to a different aspect of many-wave theory. It has been shown by Kato (1961) that an incoming spherical wave in the case of two beams is capable of exciting an extended portion of the dispersion surface. This effect results (Hattori & Kato, 1966) experimentally in hyperbolic section patterns whose appearance is governed by Bessel functions of zeroth and first order. However, identical angular intensity distributions have been obtained by Authier & Simon (1968) by means of the conceptually simpler Takagi–Taupin treatment (Takagi, 1962, 1969; Taupin, 1964). A natural extension of these calculations would be to obtain solutions that are valid for three coupled waves. Using integral equations (Bremer, 1984) we now perform such a generalization. The derived expressions can be looked upon as boundary Green functions for the wave field inside the crystal, and may for that reason find applications in analytical and numerical works. If the wave front of the incoming wave is sufficiently narrow, however, it should be possible to make a direct observation of the intensity pattern.

The three-dimensional interference pattern

The field equations

The vacuum wave entering the crystal is assumed to excite the wave field

$$\mathbf{D}(\mathbf{r}) = \sum_q \mathbf{D}_q(\mathbf{r}) \exp(-2\pi i \mathbf{k}_q \mathbf{r}), \tag{1}$$

where the crystal wave vectors $\mathbf{k}_q$ are given by

$$\mathbf{k}_q = \mathbf{k}_0 + \mathbf{q}. \tag{2}$$

Here q denotes a reciprocal-lattice point while $\mathbf{q}$ is the associated reciprocal-lattice vector.

The vector amplitudes $\{\mathbf{D}_q\}$ are decomposed along two mutually orthogonal directions defined by the polarization vectors $\{\hat{e}_{q\mu}, \mu = 1, 2\}$ (usually called $\hat{\sigma}_q$ and $\hat{\pi}_q$), *i.e.*

$$\mathbf{D}_q = \sum_\mu D_{q\mu} \hat{e}_{q\mu}. \tag{3}$$

According to the Takagi–Taupin equations for a perfect crystal (Takagi, 1969) we have

$$\partial D_{q\mu}/\partial s_q = 2i\pi K \beta_q D_{q\mu} - i\pi K \left\{ \sum_{\substack{\nu \\ p \neq q}} \chi_{q-p} (\hat{e}_{q\mu} \cdot \hat{e}_{p\nu}) D_{p\nu} \right\}, \tag{4}$$

where s_q is a coordinate along the base vector $\hat{s}_q = \mathbf{k}_q/|\mathbf{k}_q|$, $K = 1/\lambda$ is the wave number of the incoming vacuum wave, and the parameter β_q is defined (Authier, Malgrange & Tournarie, 1968) as

$$\beta_q = [|\mathbf{k}_q| - K(1 + \tfrac{1}{2}\chi_0)]/K. \tag{5}$$

The Fourier components of the electrical susceptibility, χ_q, are given by

$$\chi_q = -(r_e \lambda^2/\pi V_c) F_q. \tag{6}$$

Here r_e is the classical electron radius, V_c the unit-cell volume and F_q is the structure factor of the reflection q. Refraction and average absorption are associated with $\mathrm{Re}\{\chi_0\}$ and $\mathrm{Im}\{\chi_0\}$, respectively.

The first term on the right-hand side of (4) can always be eliminated by means of a simple redefinition of phases, *i.e.*

$$D_{q\mu} = \bar{D}_{q\mu} \exp\left\{ 2i\pi K \sum_p \beta_p s_p \right\}. \tag{7}$$

The difference between $D_{q\mu}$ and $\bar{D}_{q\mu}$ turns out to be important for the intensity distribution only in the case of incoming waves with extended wave fronts. We will use the symbol D for the wave fields everywhere when confusion cannot arise.

Up to this point we have not restricted the number of waves participating in the interaction. In what follows we will, however, limit ourselves to studying the coupling of three waves, *i.e.* $q \in (0, h, g)$. Furthermore, we will neglect terms due to coupling between the $\hat{\sigma}$ and $\hat{\pi}$ components of the waves, *i.e.*

$$\hat{e}_{q\mu} \cdot \hat{e}_{p\nu} = \hat{e}_{q\mu} \cdot \hat{e}_{p\mu} \delta_{\mu,\nu}, \tag{8}$$

where δ is the Kronecker delta symbol. The index μ is therefore dropped from now on.

Defining the parameter

$$\tau_{q-p} = (-\pi K \chi_{q-p} \hat{e}_q \cdot \hat{e}_p)^{-1}, \tag{9}$$

whose real value is equal to the extinction length, we can write the equations describing the coupling of three waves explicitly as

$$\partial D_0/\partial s_0 = i\tau_{\bar{h}}^{-1} D_h + i\tau_{\bar{g}}^{-1} D_g \tag{10a}$$

$$\partial D_h/\partial s_h = i\tau_{h-g}^{-1} D_g + i\tau_h^{-1} D_0 \tag{10b}$$

$$\partial D_g/\partial s_g = i\tau_g^{-1} D_0 + i\tau_{g-h}^{-1} D_h, \tag{10c}$$

where we have performed the transformation indicated by (7).

Integral-equation formulation and boundary conditions

The wave amplitude $D_h(s_0, s_h, s_g)$ is formally obtained from (10b) by integration

$$\begin{aligned} D_h(s_0, s_h, s_g) &= D_h[s_0, s_h^b(s_0, s_g), s_g] \\ &+ (i/\tau_{h-g}) \int_{s_h^b(s_0, s_g)}^{s_h} \mathrm{d}s_h' D_g(s_0, s_h', s_g) \\ &+ (i/\tau_h) \int_{s_h^b(s_0, s_g)}^{s_h} \mathrm{d}s_h' D_0(s_0, s_h', s_g) \end{aligned} \tag{11}$$

with corresponding expressions for D_0 and D_g. The function $s_h = s_h^b(s_0, s_g)$ describes the shape of the crystal boundary. Equation (11) is analogous to the equation used by Werner (1974) for solving the Darwin transfer equations in the two-beam case. We assume that the boundary values of D_0, D_h and D_g are known and limit the discussion to cases where there is no direct coupling between two of the three waves:

(i) $|\tau_{\pm g}| \to \infty$.

(ii) $|\tau_{\pm(h-g)}| \to \infty$.

Case (i) corresponds to $|\tau_{\bar{g}}| \gg |\tau_{\bar{h}}|$ and $|\tau_g| \gg |\tau_{g-h}|$. Case (ii) is realized when $|\tau_{h-g}| \gg |\tau_h|$ and $|\tau_{g-h}| \gg |\tau_g|$. We will only consider 'proper' three-dimensional cases where the coordinates s_0, s_h and s_g are independent. Coplanar diffraction is therefore excluded. Using the expressions corresponding to (11) for D_0 and D_g we find that D_h in case (i) fulfils

$$\begin{aligned} D_h(s_0, s_h, s_g) &= D_h[s_0, s_h^b(s_0, s_g), s_g] \\ &+ (i/\tau_h) \int_{s_h^b(s_0, s_g)}^{s_h} \mathrm{d}s_h' D_0[s_0^b(s_h', s_g), s_h', s_g] \\ &+ (i/\tau_{h-g}) \int_{s_h^b(s_0, s_g)}^{s_h} \mathrm{d}s_h' D_g[s_0, s_h', s_g^b(s_0, s_h')] \\ &- (\tau_h \tau_{\bar{h}})^{-1} \int_{s_h^b(s_0, s_g)}^{s_h} \mathrm{d}s_h' \int_{s_0^b(s_h', s_g)}^{s_0} \mathrm{d}s_0' D_h(s_0', s_h', s_g) \\ &- (\tau_{h-g} \tau_{g-h})^{-1} \int_{s_h^b(s_0, s_g)}^{s_h} \mathrm{d}s_h' \\ &\times \int_{s_g^b(s_0, s_h')}^{s_g} \mathrm{d}s_g' D_h(s_0, s_h', s_g'). \end{aligned} \tag{12}$$

In case (ii) it is more convenient to work out an equation for D_0 which takes the form

$$\begin{aligned} D_0(s_0, s_h, s_g) &= D_0[s_0^b(s_h, s_g), s_h, s_g] \\ &+ (i/\tau_{\bar{h}}) \int_{s_0^b(s_h, s_g)}^{s_0} \mathrm{d}s_0' D_h[s_0', s_h^b(s_0', s_g), s_g] \\ &+ (i/\tau_{\bar{g}}) \int_{s_0^b(s_h, s_g)}^{s_0} \mathrm{d}s_0' D_g[s_0', s_h, s_g^b(s_0', s_h)] \\ &- (\tau_h \tau_{\bar{h}})^{-1} \int_{s_0^b(s_h, s_g)}^{s_0} \mathrm{d}s_0' \int_{s_h^b(s_0', s_g)}^{s_h} \mathrm{d}s_h' D_0(s_0', s_h', s_g) \\ &- (\tau_g \tau_{\bar{g}})^{-1} \int_{s_0^b(s_h, s_g)}^{s_0} \mathrm{d}s_0' \int_{s_g^b(s_0', s_h)}^{s_g} \mathrm{d}s_g' D_0(s_0', s_h, s_g'). \end{aligned} \tag{13}$$

The boundary-value Green functions for the wave fields are obtained by locating a point source at the origin of the coordinate system defined by the base vectors $\hat{s}_0$, $\hat{s}_h$ and $\hat{s}_g$ (Fig. 1). The boundary conditions are then given by

$$D_0[s_0^b(s_h, s_g), s_h, s_g] = \delta(s_h)\delta(s_g) \tag{14a}$$

$$D_h[s_0, s_h^b(s_0, s_g), s_g] = 0 \tag{14b}$$

$$D_g[s_0, s_h, s_g^b(s_0, s_g)] = 0. \tag{14c}$$

A discussion of geometrical factors which are to be included in (14a) in case of an incoming plane wave will be given later. Equations (14) imply that the wave fields outside the pyramid defined by $\hat{s}_0$, $\hat{s}_h$ and $\hat{s}_g$ are zero. This is a natural extension of the analogous arguments put forward for the two-wave

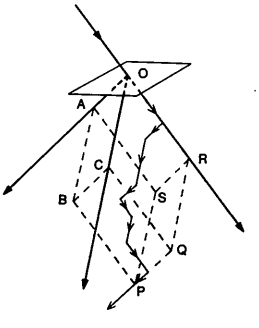

Fig. 1. The origin of the applied coordinate system is located at O and the narrow incoming wave points in the **OR** direction. The unit vectors $\hat{s}_0$, $\hat{s}_h$ and $\hat{s}_g$ are parallel to **OR**, **OC** and **OA**.

case (Kato, 1976) since it is impossible for photons to reach this part of the crystal through scattering/rescattering events. In general, the lower limits of integration in (12) and (13) have to be replaced by s_q^L $(q=0, h, g)$, where, for instance,

$$s_0^L = s_0^L(s_h, s_g) = \max\{0, s_0^b(s_h, s_g)\}. \tag{15}$$

Restricting ourselves to 'normal' Laue diffraction we put $s_q^L = 0$.

Combining the results above we arrive at the following integral equation for the wave fields:

Case (i) $|\tau_{\pm g}| \to \infty$.

$$\begin{aligned} D_h(s_0, s_h, s_g) &= (i/\tau_h)\delta(s_g) \\ &\quad -(\tau_h\tau_{\bar{h}})^{-1}\int_0^{s_h} ds_h' \int_0^{s_0} ds_0'\, D_h(s_0', s_h', s_g) \\ &\quad -(\tau_{h-g}\tau_{g-h})^{-1}\int_0^{s_h} ds_h' \int_0^{s_g} ds_g'\, D_h(s_0, s_h', s_g'). \end{aligned} \tag{16}$$

Case (ii) $|\tau_{\pm(h-g)}| \to \infty$.

$$\begin{aligned} D_0(s_0, s_h, s_g) &= \delta(s_h)\delta(s_g) \\ &\quad -(\tau_h\tau_{\bar{h}})^{-1}\int_0^{s_0} ds_0' \int_0^{s_h} ds_h'\, D_0(s_0', s_h', s_g) \\ &\quad -(\tau_g\tau_{\bar{g}})^{-1}\int_0^{s_0} ds_0' \int_0^{s_g} ds_g'\, D_0(s_0', s_h, s_g'). \end{aligned} \tag{17}$$

Let P be an arbitrary point inside the pyramid defined by $\hat{s}_0$, $\hat{s}_h$ and $\hat{s}_g$, *cf.* Fig. 1. It follows from (16) and (17) that the fields D_h (i) and D_0 (ii) are given by integrals over the parallelograms *PBAS*, *PQRS* and *PQCB*. In effect, then, the whole volume of the oblique prism *OABCPQRS* contributes to the fields at *P*.

Solutions for the wave fields

Using the boundary conditions (14) we now work out general solutions of (12) and (13) by means of an iterative procedure.

Case (i). Equation (16) can be rewritten as

$$\begin{aligned} D_h(s_0, s_h, s_g) &= (i/\tau_h)\delta(s_g) + \{-(\tau_h\tau_{\bar{h}})^{-1}L_{h0} \\ &\quad -(\tau_{h-g}\tau_{g-h})^{-1}L_{hg}\}D_h(s_0, s_h, s_g), \end{aligned} \tag{18}$$

where the linear operators L_{h0} and L_{hg} are defined by

$$L_{h0}\{D_h(s_0, s_h, s_g)\} = \int_0^{s_h} ds_h' \int_0^{s_0} ds_0'\, D_h(s_0', s_h', s_g) \tag{19a}$$

$$L_{hg}\{D_h(s_0, s_h, s_g)\} = \int_0^{s_h} ds_h' \int_0^{s_g} ds_g'\, D_h(s_0, s_h', s_g'). \tag{19b}$$

The wave field D_h thus becomes

$$\begin{aligned} D_h(s_0, s_h, s_g) &= (i/\tau_h)[1 + (\tau_h\tau_{\bar{h}})^{-1}L_{h0} \\ &\quad +(\tau_{h-g}\tau_{g-h})^{-1}L_{hg}]^{-1}\delta(s_g), \end{aligned} \tag{20a}$$

which may be expanded as

$$\begin{aligned} D_h(s_0, s_h, s_g) &= (i/\tau_h)\sum_{n=0}^{\infty}(-1)^n[(\tau_h\tau_{\bar{h}})^{-1}L_{h0} \\ &\quad +(\tau_{h-g}\tau_{g-h})^{-1}L_{hg}]^n\delta(s_g) \\ &= (i/\tau_h)\sum_{n=0}^{\infty}\sum_{m=0}^{\infty}\binom{n+m}{m}(-1)^{n+m} \\ &\quad \times(\tau_h\tau_{\bar{h}})^{-n}(\tau_{h-g}\tau_{g-h})^{-m}L_{h0}^n L_{hg}^m\,\delta(s_g). \end{aligned} \tag{20b}$$

We have used the binomial theorem and $L_{h0}^n L_{hg}^m\,\delta(s_g)$ means n and m successive applications of the operators L_{h0} and L_{hg} on the Dirac function. The result of this operation is

$$\begin{aligned} L_{h0}^n L_{hg}^m\,\delta(s_g) &= (n!)^{-2}(s_0 s_h)^n\delta(s_g)\,\delta_{m,0} \\ &\quad +(n!)^{-1}s_0^n[(n+m)!]^{-1}s_h^{n+m} \\ &\quad \times[(m-1)!]^{-1}s_g^{m-1}(1-\delta_{m,0}). \end{aligned} \tag{21}$$

Combining (20*b*) and (21) we find that the sum over n and m represents a product of two Bessel functions of zeroth and first order:

$$\begin{aligned} D_h(s_0, s_h, s_g) &= (i/\tau_h)\{J_0[2(\tau_h\tau_{\bar{h}})^{-1/2}(s_0 s_h)^{1/2}]\delta(s_g) \\ &\quad -(\tau_{h-g}\tau_{g-h})^{-1/2}(s_h/s_g)^{1/2} \\ &\quad \times J_0[2(\tau_h\tau_{\bar{h}})^{-1/2}(s_0 s_h)^{1/2}] \\ &\quad \times J_1[2(\tau_{h-g}\tau_{g-h})^{-1/2}(s_h s_g)^{1/2}]\}. \end{aligned} \tag{22a}$$

Knowing D_h, we obtain D_0 from (10*a*) and D_g from (10*c*):

$$\begin{aligned} D_0(s_0, s_h, s_g) &= \delta(s_h)\,\delta(s_g) - (\tau_h\tau_{\bar{h}})^{-1/2}(s_0/s_h)^{1/2} \\ &\quad \times J_1[2(\tau_h\tau_{\bar{h}})^{-1/2}(s_0 s_h)^{1/2}]\,\delta(s_g) \\ &\quad +(\tau_h\tau_{\bar{h}}\tau_{h-g}\tau_{g-h})^{-1/2}(s_0/s_g)^{1/2} \\ &\quad \times J_1[2(\tau_h\tau_{\bar{h}})^{-1/2}(s_0 s_h)^{1/2}] \\ &\quad \times J_1[2(\tau_{h-g}\tau_{g-h})^{-1/2}(s_h s_g)^{1/2}]; \end{aligned} \tag{22b}$$

$$\begin{aligned} D_g(s_0, s_h, s_g) &= -(\tau_h\tau_{g-h})^{-1}J_0[2(\tau_h\tau_{\bar{h}})^{-1/2}(s_0 s_h)^{1/2}] \\ &\quad \times J_0[2(\tau_{h-g}\tau_{g-h})^{-1/2}(s_h s_g)^{1/2}]. \end{aligned} \tag{22c}$$

The results in (22) should be multiplied by the unit step functions $\theta(s_0)\theta(s_h)\theta(s_g)$ in order to make it clear that the wave fields are zero outside the pyramid defined by the unit vectors $\hat{s}_0$, $\hat{s}_h$ and $\hat{s}_g$.

Case (ii). The formal solution of (17) is

$$D_0(s_0, s_h, s_g) = \sum_{n=0}\sum_{m=0} \binom{n+m}{m}(-1)^{n+m} \times (\tau_h\tau_{\bar{h}})^{-n}(\tau_g\tau_{\bar{g}})^{-m} L_{0h}^n L_{0g}^m\, \delta(s_h)\, \delta(s_g). \quad (23)$$

Using the result

$$\begin{aligned} L_{0h}^n L_{0g}^m\, \delta(s_h)\, \delta(s_g) &= \delta(s_h)\, \delta(s_g)\, \delta_{n,0}\, \delta_{m,0} \\ &+ (n!)^{-1} s_0^n [(n-1)!]^{-1} s_h^{n-1}\, \delta(s_g)(1-\delta_{n,0})\, \delta_{m,0} \\ &+ (m!)^{-1} s_0^m [(m-1)!]^{-1} s_g^{m-1}\, \delta(s_h) \\ &\times (1-\delta_{m,0})\, \delta_{n,0} \\ &+ [(n+m)!]^{-1} s_0^{n+m} [(n-1)!]^{-1} s_h^{n-1} \\ &\times [(m-1)!]^{-1} s_g^{m-1} (1-\delta_{n,0})(1-\delta_{m,0}), \end{aligned} \quad (24)$$

we obtain for the field D_0:

$$\begin{aligned} D_0(s_0, s_h, s_g) &= \delta(s_h)\, \delta(s_g) - (\tau_g\tau_{\bar{g}})^{-1/2}(s_0/s_g)^{1/2} \\ &\times J_1[2(\tau_g\tau_{\bar{g}})^{-1/2}(s_0 s_g)^{1/2}]\, \delta(s_h) \\ &- (\tau_h\tau_{\bar{h}})^{-1/2}(s_0/s_h)^{1/2} \\ &\times J_1[2(\tau_h\tau_{\bar{h}})^{-1/2}(s_0 s_h)^{1/2}]\, \delta(s_g) \\ &+ (\tau_h\tau_{\bar{h}}\tau_g\tau_{\bar{g}})^{-1/2} s_0 (s_h s_g)^{-1/2} \\ &\times J_1[2(\tau_h\tau_{\bar{h}})^{-1/2}(s_0 s_h)^{1/2}] \\ &\times J_1[2(\tau_g\tau_{\bar{g}})^{-1/2}(s_0 s_g)^{1/2}]. \end{aligned} \quad (25a)$$

From (10*b*) we find

$$\begin{aligned} D_h(s_0, s_h, s_g) &= (i/\tau_h)\{J_0[2(\tau_h\tau_{\bar{h}})^{-1/2}(s_0 s_h)^{1/2}]\, \delta(s_g) \\ &- (\tau_g\tau_{\bar{g}})^{-1/2}(s_0/s_g)^{1/2} \\ &\times J_0[2(\tau_h\tau_{\bar{h}})^{-1/2}(s_0 s_h)^{1/2}] \\ &\times J_1[2(\tau_g\tau_{\bar{g}})^{-1/2}(s_0 s_g)^{1/2}]\}. \end{aligned} \quad (25b)$$

A completely symmetrical expression for D_g can be derived from (10*c*):

$$\begin{aligned} D_g(s_0, s_h, s_g) &= (i/\tau_g)\{J_0[2(\tau_g\tau_{\bar{g}})^{-1/2}(s_0 s_g)^{1/2}]\, \delta(s_h) \\ &- (\tau_h\tau_{\bar{h}})^{-1/2}(s_0/s_h)^{1/2} \\ &\times J_0[2(\tau_g\tau_{\bar{g}})^{-1/2}(s_0 s_g)^{1/2}] \\ &\times J_1[2(\tau_h\tau_{\bar{h}})^{-1/2}(s_0 s_h)^{1/2}]\}. \end{aligned} \quad (25c)$$

Again, the fields are zero if at least one of the coordinates becomes negative.

Discussion

Transition to two waves

The singular term $\delta(s_h)\delta(s_g)$ in the expressions for D_0 represents a wave that is transmitted without being scattered. Clearly, this is a result of modelling the exciting wave with a vanishing wave-front area. Furthermore, as is evident from (22) and (25), the Green functions for the wave fields have terms that are proportional to $\delta(s_h)$ or $\delta(s_g)$. These terms have to be associated with two-wave diffraction, which takes place within the planes spanned by $\hat{s}_0$ and $\hat{s}_g$, or $\hat{s}_0$ and $\hat{s}_h$, respectively. In order to show more explicitly that the usual two-wave solution for D_0 and D_h is included in (22) and (25), we now weaken the coupling to the third wave D_g. This is done by permitting $|\tau_{\pm(h-g)}| \to \infty$ {case (i)} or $|\tau_{\pm g}| \to \infty$ {case (ii)}. In addition, however, we have to replace the applied point source with a line source. The published expressions for two-beam intensities (Kato, 1974; Authier & Simon, 1968) are implicitly based on the presence of a narrow long slit oriented normal to the $s_0 s_h$ plane. In practice, the replacement is achieved by letting $\delta(s_g) \to 1$. We obtain the well known results

$$D_h(s_0, s_h) = (i/\tau_h) J_0[2(\tau_h\tau_{\bar{h}})^{-1/2}(s_0 s_h)^{1/2}] \quad (26a)$$

and

$$\begin{aligned} D_0(s_0, s_h) &= \delta(s_h) - (\tau_h\tau_{\bar{h}})^{-1/2}(s_0/s_h)^{1/2} \\ &\times J_1[2(\tau_h\tau_{\bar{h}})^{-1/2}(s_0 s_h)^{1/2}], \end{aligned} \quad (26b)$$

which describe the spatial variation of two coupled waves.

The intensity pattern

The intensity $I_q = D_q D_q^*$ inside the pyramid (Fig. 1) is given by the non-singular parts of (22) and (25). The results of simulating I_h for the cases (i) and (ii) in a centrosymmetric crystal are shown in Fig. 2. In order to show more clearly the position of the maxima and minima we exhibit not the intensity itself but rather its logarithmic variation $[\ln(I_h)]$. Fig. 2(*a*) corresponds to (22*a*) while Fig. 2(*b*) is based on (25*b*). We have assumed that $\hat{s}_0$, $\hat{s}_h$ and $\hat{s}_g$ are perpendicular to each other and $OA = OC = OR = 5|\tau_h|$ with $|\tau_h| = 1$ (arbitrary units). Other parameters are $|\tau_{g-h}|/|\tau_h| = 3/2(a)$ and $|\tau_g|/|\tau_h| = 3/2(b)$. Absorption is neglected and black portions correspond to areas with high intensity. The influence of the wave D_g on D_h is clearly seen in both (*a*) and (*b*). For the sake of comparison we have included the two-wave result based on (26*a*) in (*c*). It should be emphasized, however, that the intensity patterns shown in Figs. 2(*a*) and (*b*) are not obtained by superposition of two-wave expressions. In the limits of no direct interaction between two of the three waves the products of two-wave expressions determine the fringes. Furthermore, in the same limits the intensity patterns will not contain information related to the invariant phase of the product of the structure factors involved (*e.g.* Hart & Lang, 1961; Høier & Aanestad, 1981).

Transition to plane waves

The case of an incoming plane wave with field amplitude $D_0^{(e)}$ can be treated by decomposing the

wave into a uniform distribution of δ pulses. The field density, $d_0(S)$, at a point S on the entrance surface of the crystal takes the form

$$d_0(S) = D_0^{(e)}\,\delta[t_1 - t_1(S)]\,\delta[t_2 - t_2(S)], \quad (27)$$

where t_1 and t_2 are coordinates along unit vectors perpendicular to the propagation direction of the incoming wave $\hat{s}_0$. (It is convenient to use the polarization vectors $\{\hat{e}_{0\mu}\}$ as unit vectors associated with $\hat{s}_0$.) In the oblique crystal system (s_0, s_h, s_g) the density $d_0(S)$ transforms into

$$d_0(S) = D_0^{(e)} J\,\delta[s_h - s_h(S)]\,\delta[s_g - s_g(S)], \quad (28)$$

where

$$J = |\partial(s_h, s_g)/\partial(t_1, t_2)| \quad (29)$$

is the Jacobian of the actual coordinate transformation.

The fields $\{\bar{D}_q\}$ due to the point source $\delta(s_h)\,\delta(s_g)$ are given by (22), (25). The field amplitude D_q at a point P inside the crystal due to a source at the point S thus becomes

$$\begin{aligned} D_q(P \leftarrow S) = \bar{D}_q[&s_0(P) - s_0(S),\ s_h(P) - s_h(S),\\ &s_g(P) - s_g(S)]\\ &\times \exp\left\{2\pi i K \sum_p \beta_p[s_p(P) - s_p(S)]\right\}\\ &\times \theta[s_0(P) - s_0(S)]\,\theta[s_h(P) - s_h(S)]\\ &\times \theta[s_g(P) - s_g(S)], \end{aligned} \quad (30)$$

where $p, q \in \{0, h, g\}$.

The field $D_q(P)$ due to the incoming plane wave is obtained by integrating (30) over the entrance surface.

$$D_q(P) = D_0^{(e)} J \int_S \mathrm{d}\mathbf{S}.\hat{s}_0 D_q(P \leftarrow S). \quad (31)$$

In (31), dS is a vector element of the entrance surface area directed along the inward drawn normal vector. The simple case of a plane surface is illustrated in Fig. 3. Only photons entering the triangular area ABC are capable of contributing to the intensity at P when following arbitrary paths along the $\hat{s}_0$, $\hat{s}_h$ and $\hat{s}_g$ directions. The prism of Fig. 1 is henceforth transformed into a pyramid.

The field D_q is generally a function of two external divergency angles ε_1 and ε_2 which define the position of the incident wave vector relative to the Laue point (Pinsker, 1978; Høier & Marthinsen, 1983). We now

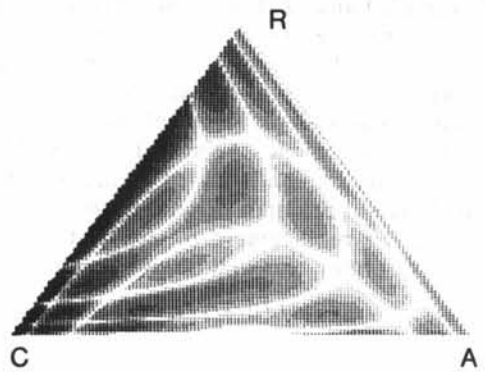

(*a*)

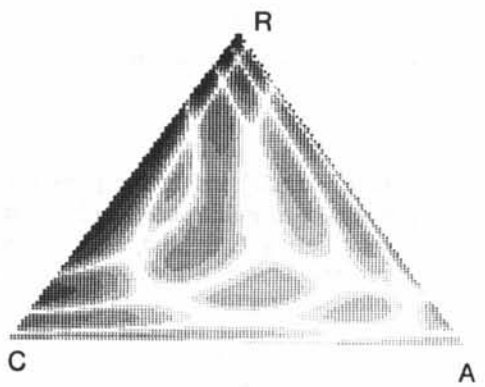

(*b*)

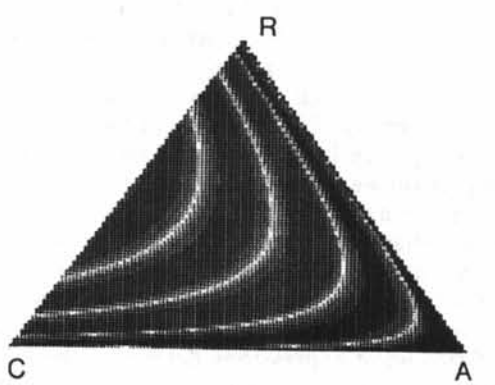

(*c*)

Fig. 2. Modulation of I_h (logarithmic scale) owing to the presence of a third wave D_g. The letters denote the same position as in Fig. 1. (See text.) A slight geometrical distortion ($CR < CA$) is introduced for technical reasons. (*a*) Indirect coupling between D_0 and D_g. (*b*) Direct coupling between D_0 and D_g. (*c*) Two-wave *Pendellösung* fringes. In the limit of negligible direct coupling between two of the three beams the intensity patterns are given by products (not superpositions) of two-wave expressions.

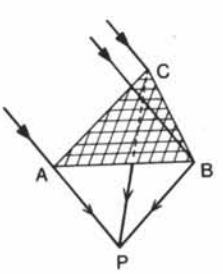

Fig. 3. The extreme case of a plane wave entering the crystal. The triangular contour ABC shows that part of the surface region that is capable of contributing to the wave field at P (see text) ($\hat{s}_0 \| \mathbf{AP}$, $\hat{s}_h \| \mathbf{CP}$ and $\hat{s}_g \| \mathbf{BP}$).

let P represent a point on the exit surface of the crystal. The integrated intensity, $I_q(P)$, emerging from P is

$$I_q(P) = \int \mathrm{d}\varepsilon_1 \int \mathrm{d}\varepsilon_2 |D_q(\varepsilon_1, \varepsilon_2)|^2. \quad (32)$$

The integrated power, P_q, is then obtained by integrating (32) over the exit surface

$$P_q = \int_P \mathrm{d}\mathbf{P}.\hat{s}_q I_q(P). \quad (33)$$

The surface element d**P** points in the direction of the outward drawn normal.

It is difficult to perform analytically the integrations in (31), (32) and (33) and only numerical solutions are feasible for arbitrary crystal shapes.

Concluding remarks

The Takagi–Taupin equations have been examined for three coupled waves in the case of Laue diffraction. When the coupling constant $1/\tau_{\pm g}$ or $1/\tau_{\pm(h-g)}$ becomes negligible it is possible to use integral equation techniques to obtain the boundary-value Green functions for the wave fields. The solutions, excluding any singular terms, may be taken as approximate expressions for the fields excited by a transversally limited wave packet when keeping away from the surface region and the $s_0 s_h$ and the $s_0 s_g$ planes. To the author's knowledge no experimental study of the fringes generated by three indirectly coupled waves has been published. In principle, it should be possible to confirm the spatial behaviour of the intensities $I_q \sim D_q D_q^*$ by intercepting a beam with the aid of a small pin hole or, alternatively, by locating a point source close to the surface of the crystal. In the case of an incident wave with an extended wave front, the intensity can be calculated by integrating the Green functions over the entrance surface allowing for the proper variation in amplitude of the incident wave.

References

AUTHIER, A., MALGRANGE, C. & TOURNARIE, M. (1968). *Acta Cryst.* A**24**, 126–136.

AUTHIER, A. & SIMON, D. (1968). *Acta Cryst.* A**24**, 517–526.

BREMER, J. (1984). *Acta Cryst.* A**40**, 283–291.

CHANG, S.-L. (1984). *Multiple Diffraction of X-rays in Crystals.* Berlin: Springer.

HART, M. & LANG, A. R. (1961). *Phys. Rev. Lett.* **7**, 120–121.

HATTORI, H. & KATO, N. (1966). *J. Phys. Soc. Jpn*, **21**, 1772–1777.

HØIER, R. & AANESTAD, A. (1981). *Acta Cryst.* A**37**, 787–794.

HØIER, R. & MARTHINSEN, K. (1983). *Acta Cryst.* A**39**, 854–860.

KATO, N. (1961). *Acta Cryst.* **14**, 526–532, 627–636.

KATO, N. (1974). In *X-ray diffraction*, edited by L. V. AZAROFF, pp. 176–438. New York: McGraw-Hill.

KATO, N. (1976). *Acta Cryst.* A**32**, 453–457.

PINSKER, Z. G. (1978). *Dynamical Scattering of X-rays in Crystals.* Berlin: Springer.

POST, B. (1983) *Acta Cryst.* A**39**, 711–718.

TAKAGI, S. (1962). *Acta Cryst.* **15**, 1311–1313.

TAKAGI, S. (1969). *J. Phys. Soc. Jpn*, **26**, 1239–1253.

TAUPIN, D. (1964). *Bull. Soc. Fr. Minéral. Cristallogr.* **87**, 469–511.

WERNER, S. A. (1974). *J. Appl. Phys.* **45**, 3246–3254.

Acta Cryst. (1986). A**42**, 197–202

Statistical Geometry. IV. Maximum-Entropy-Based Extension of Multiple Isomorphously Phased X-ray Data to 4 Å Resolution for α-Lactalbumin

BY STEPHEN W. WILKINS*

Laboratory of Molecular Biophysics, Department of Zoology, University of Oxford, Oxford OX1 3QU, England and CSIRO, Division of Chemical Physics, PO Box 160, *Clayton, Victoria* 3168, *Australia*

AND DAVID STUART

Laboratory of Molecular Biophysics, Department of Zoology, University of Oxford, Oxford OX1 3QU, England

(*Received* 26 *July* 1985; *accepted* 20 *December* 1985)

Abstract

The simplest level of the statistical geometric (SG) or maximum-entropy (ME) approach to X-ray structure refinement is applied to the task of trying to extend the resolution of electron-density maps for a small protein (α-lactalbumin). The refinement was started from X-ray structure factor data to 4 Å resolution, which had been phased by multiple isomorphous replacement (MIR), and it was found that, even at this simple level, the ME-based approach yields a significant improvement in the maps and gives encouragement to the more general applications of these methods.

* Permanent address: CSIRO, Australia.

0108-7673/86/030197-06$01.50